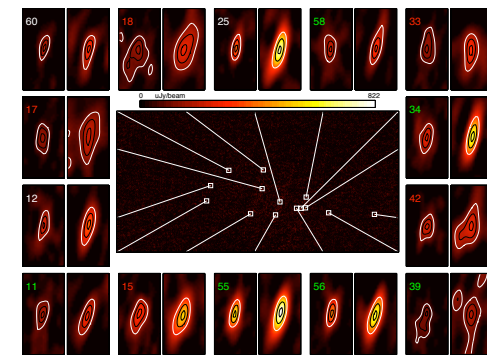
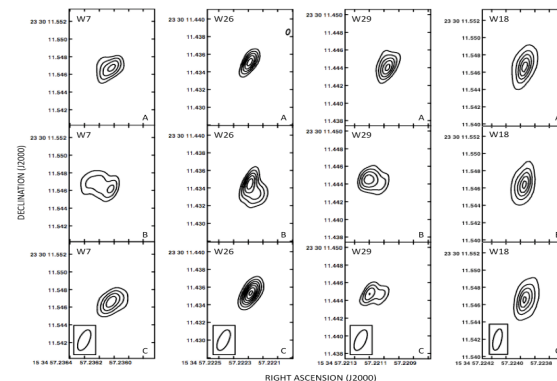




Compact source resolution and rapid variability in Arp220



Fabien Batejat
Onsala Space Observatory





Collaborators

- John Conway, Onsala
- Philip J. Diamond, Jodrell Bank
- Rodrigo Parra, CONICYT, Santiago
- Colin J. Lonsdale, Haystack, MIT
- Carol J. Lonsdale, IPAC, Caltech



Outline

- Who is Arp220? Why is it interesting?
- HSA 2cm and global VLBI 3.6cm observations
 - Source resolution, sizes, classes...
 - Luminosity – Diameter relation
- Recent global VLBI 6cm monitoring
 - New detections
 - Exotic objects
- Summary

ARP220: who is it?



Picture by Hubble Space Telescope

- Merging galaxies
- Closest ULIRG
 $77\text{Mpc} - L_{\text{fir}} > 10^{12}L_0$
- More typical of SF galaxies at $z = 1$ & similar star-formation density per unit area as $z = 6$ proto-galaxies



ARP220: why?



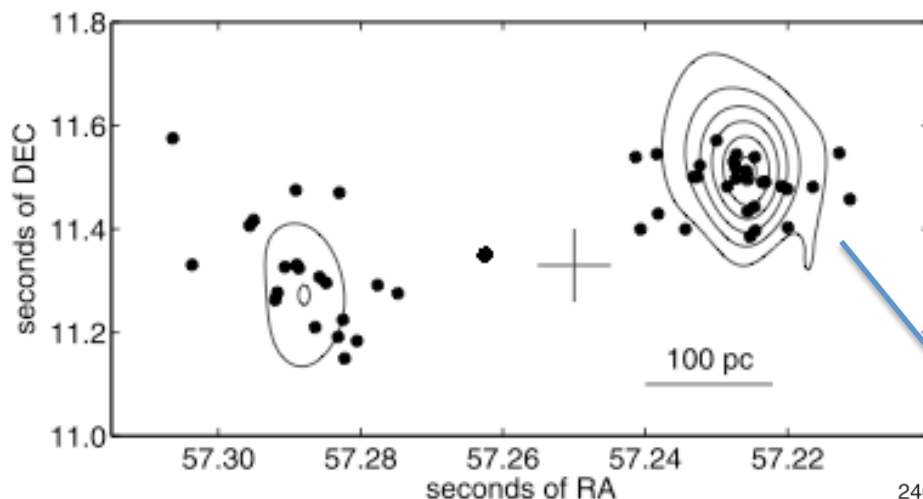
Picture by Hubble Space Telescope

- SNe and SNRs as **probes**:
 - for stellar evolution in dense environment
 - of CSM & ISM pressure and density
- SNe rate/types:
 - to **constrain top end of IMF** in regions with 100's – 1000's magnitudes of optical extinction
- Better understand **ULIRGs**:
 - just scaled up versions of disk star-formation?
 - fundamentally different?

ARP220: VLBI compact sources

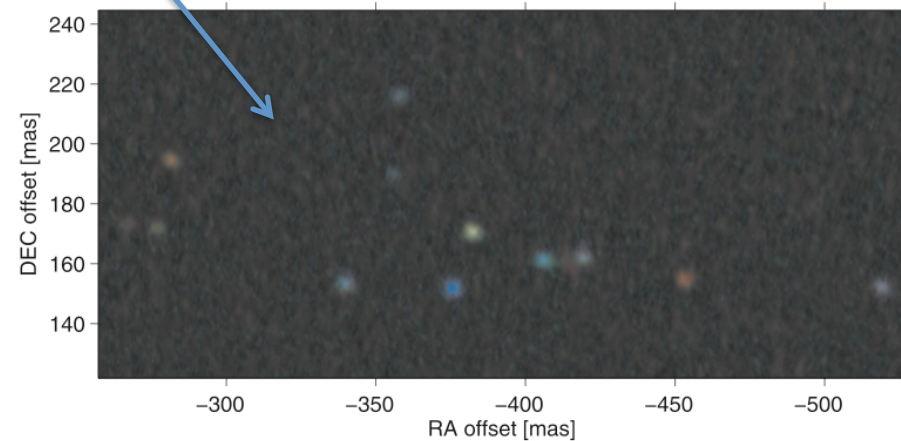


Starburst revealed at 18cm by Smith et al 1998

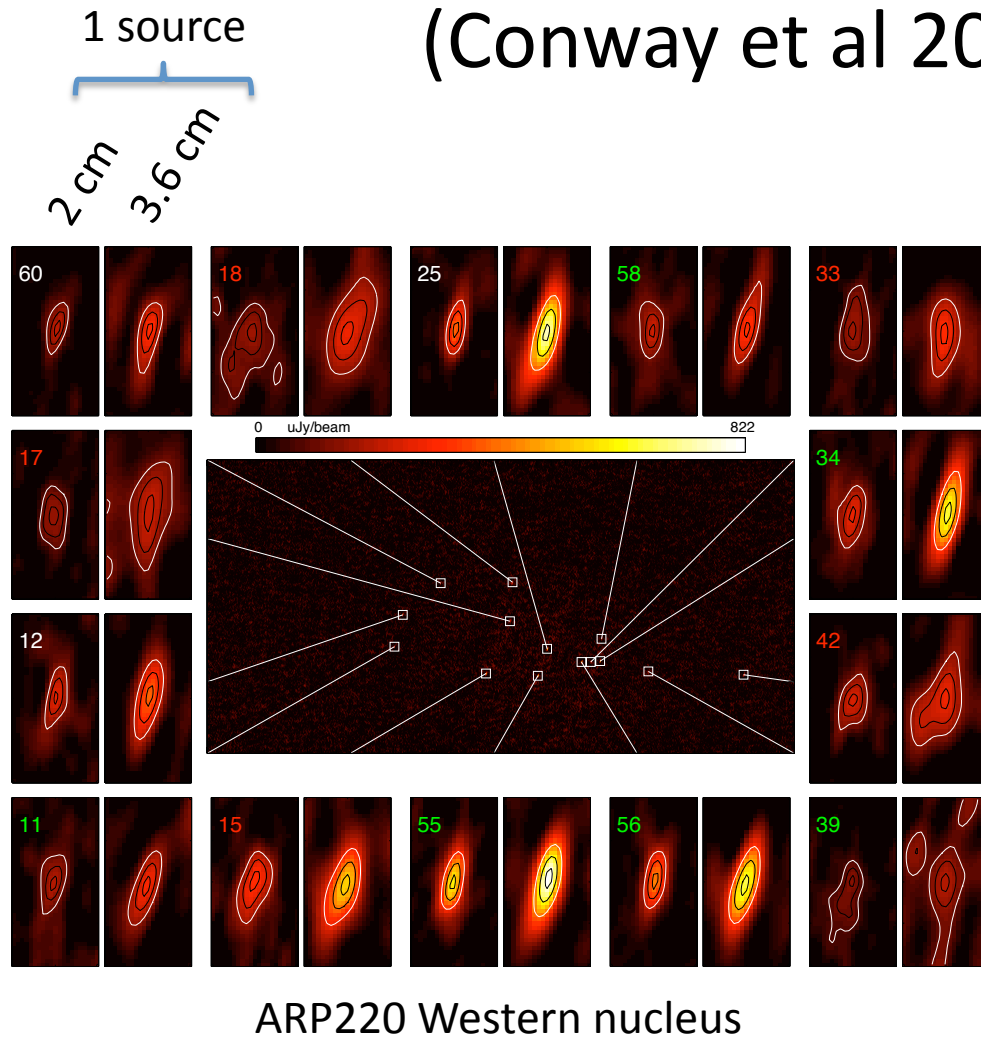


Spots: 18cm compact VLBI sources (Lonsdale et al 2006)
Contours: **first higher frequency** 6cm low resolution VLBI (Parra et al 2005)

Parra et al (2007), high-resolution multi-frequency VLBI observations.
Compact sources likely mixture of SNe/SNRs.



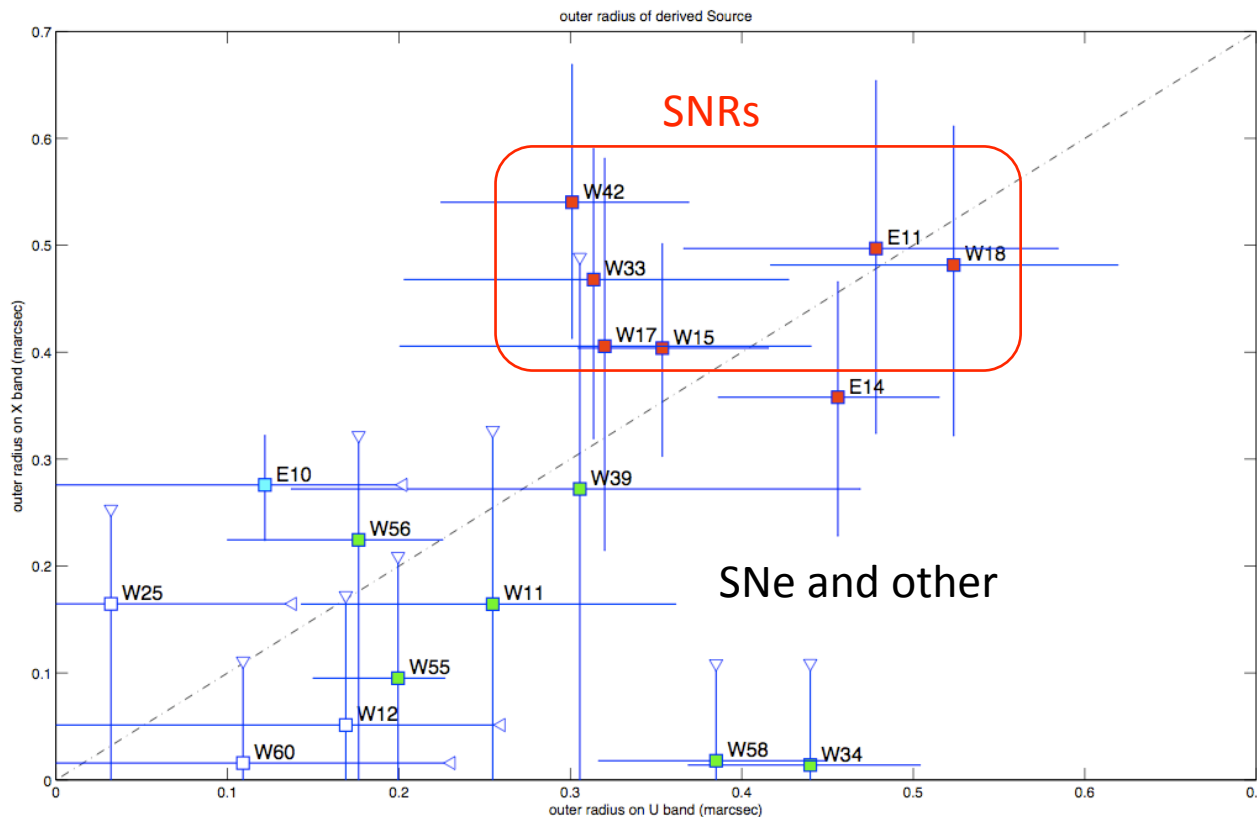
Dec 2006, 2cm and 3.6cm (Conway et al 2010)



- 17 detections:
 - 13 resolved at @ 2 cm
 - 8 resolved at @ 3.6 cm
 - 7 resolved @ 2 & 3.6 cm
 - 3 sources unresolved

HSA 2cm
Global VLBI 3.6cm

Source sizes



Source sizes range:

0.1 pc → 0.4 pc

LL source ages:

0 → 15 years

UL source exp. velocities:

9 000 → 80 000 km.s⁻¹

Red sources resolved at both bands, green only at 2cm, blue only at 3.6cm.

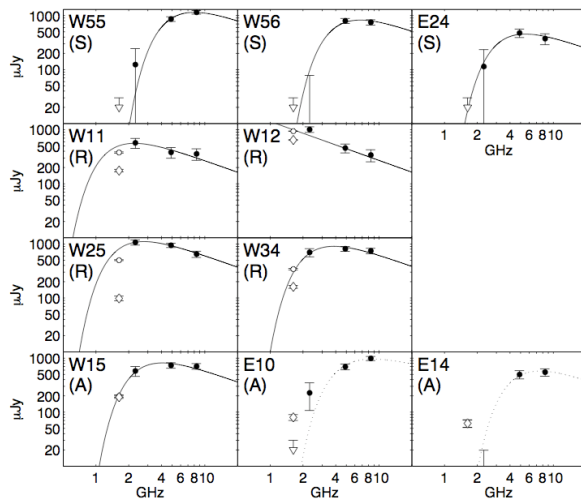
- All high frequency detected SNR are resolved (with sizes $d > 0.27\text{pc}$)
- One SN (E14) resolved at both bands, has size $d = 0.30\text{pc}$, rest $d < 0.20\text{pc}$



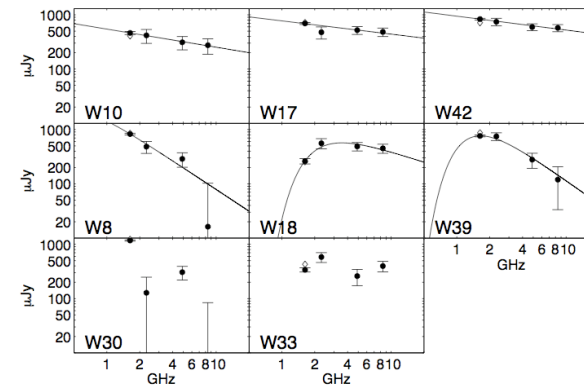
Source class

New sources

Spectra:



Long-lived sources



**Power law synchrotron
and free-free
cutoff $v > 1.6\text{GHz}$**

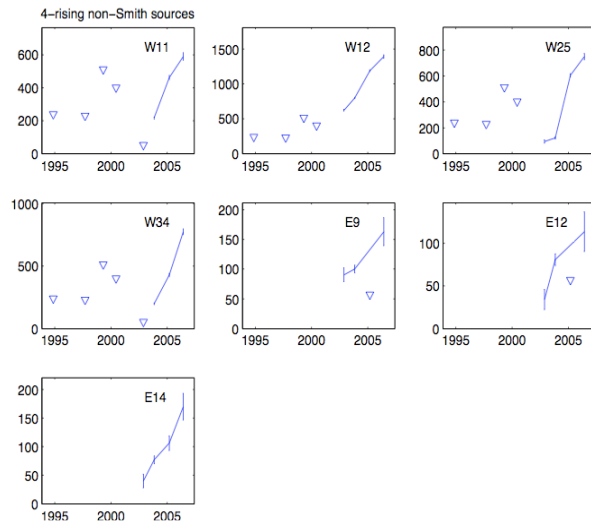
**Straight spectra with
turnover at $v < 1.6\text{GHz}$**



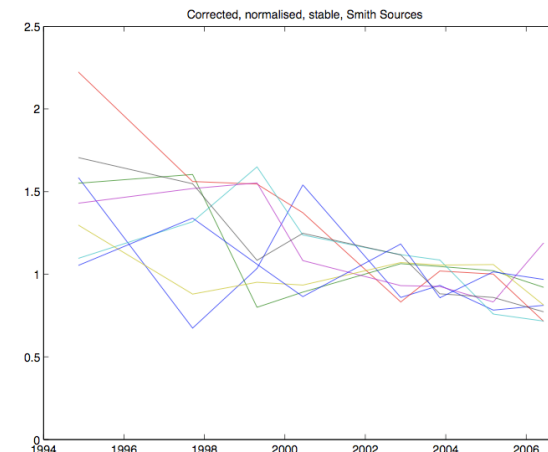
Source class

Light curves:

New sources



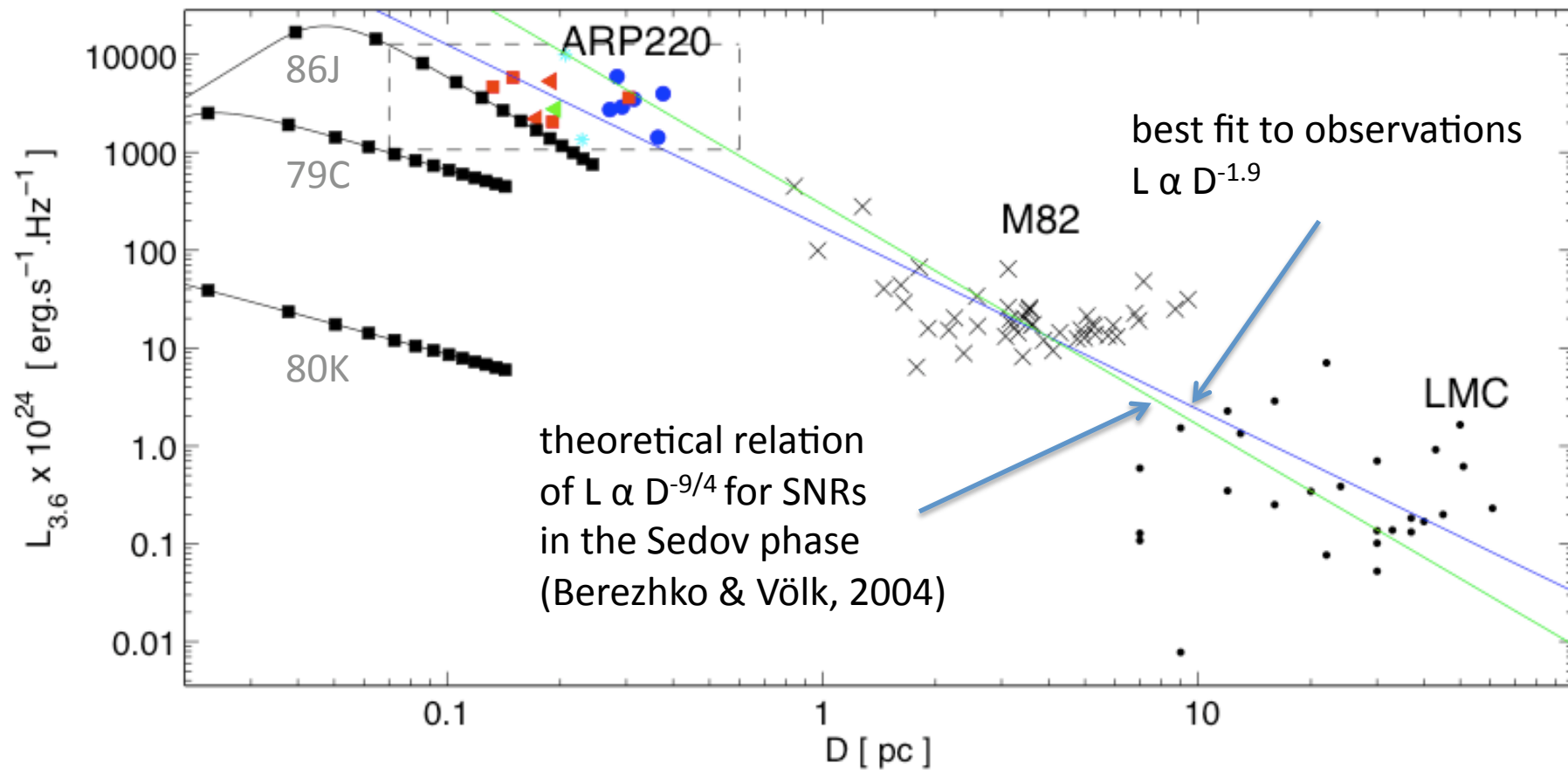
Long-lived sources



Rapidly rising sources
at 18cm

**known since 1995
decrease at 4%/year
on average**

Luminosity – Diameter relation





Berezhko and Völk (2004) model

- Similar to other models e.g. Huang et al (1994)
- Pressure in post shock shells balances ram pressure:

$$P_c \approx \rho_{ISM} V_s^2$$

- Streaming instability increases B field upstream which is then compressed and converted into magnetic energy density in the radio emitting shell:

$$B^2 / 8\pi = 0.01 P_c$$

- So $B \propto V_s$ and in the Sedov phase:

$$V_s \propto D^{-3/2}$$



Berezhko and Völk (2004) model

Remember:

$$\begin{aligned}P_c &\approx \rho_{ISM} V_S^2 \\B^2 / 8\pi &= 0.01 P_c \\V_S &\propto D^{-3/2}\end{aligned}$$

- Hence we have:

$$B \propto D^{-3/2}$$

- Synchrotron emissivity per relativistic electron in our case is:

$$\varepsilon \propto B^{3/2}$$

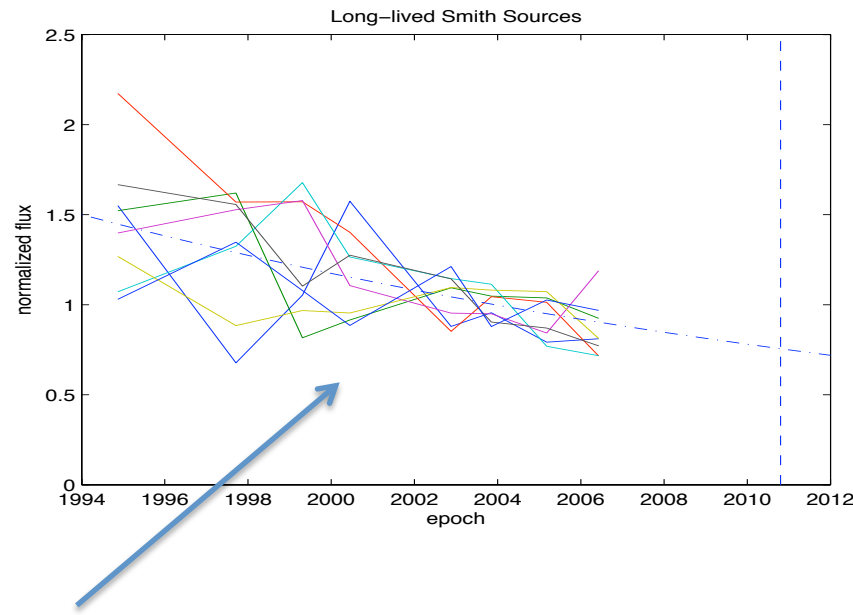
- In Sedov phase the number of relativistic electrons is fixed, so radio luminosity obeys:

$$L \propto D^{-9/4}$$

Other evidence for L-D relationship



Alternative model by Thomson et al (2009):
- claims internal B-field is B_{ISM} increased by a factor 3-6
- predicts a constant radio luminosity versus size in the Sedov phase



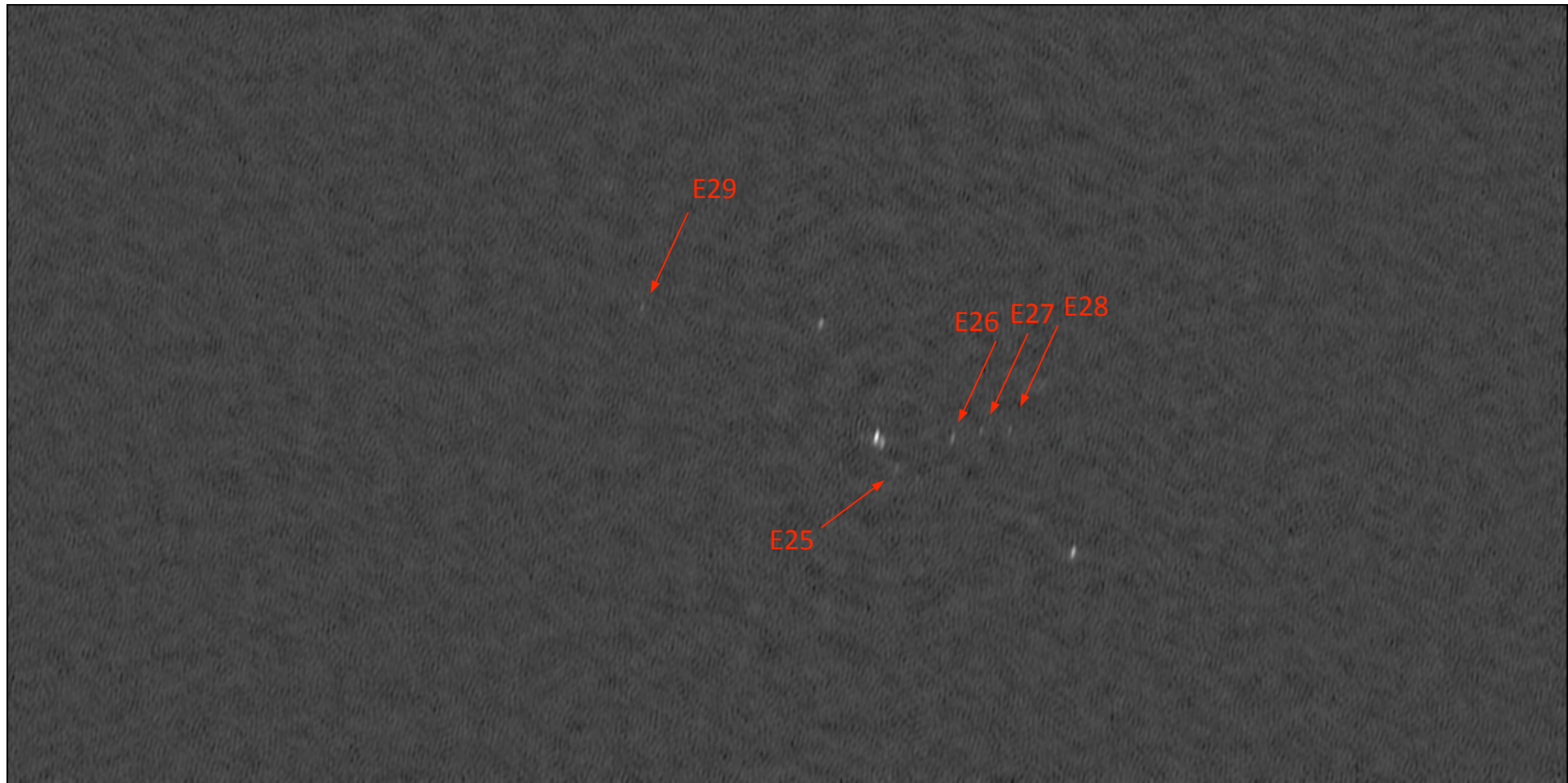
In Arp220 18cm **SNR flux decline of 4%/yr consistent with Berezhko & Völk 2004 model** if D expands 2%/yr and confirms the idea of B field changing with the source size.

Recent global VLBI 6cm monitoring



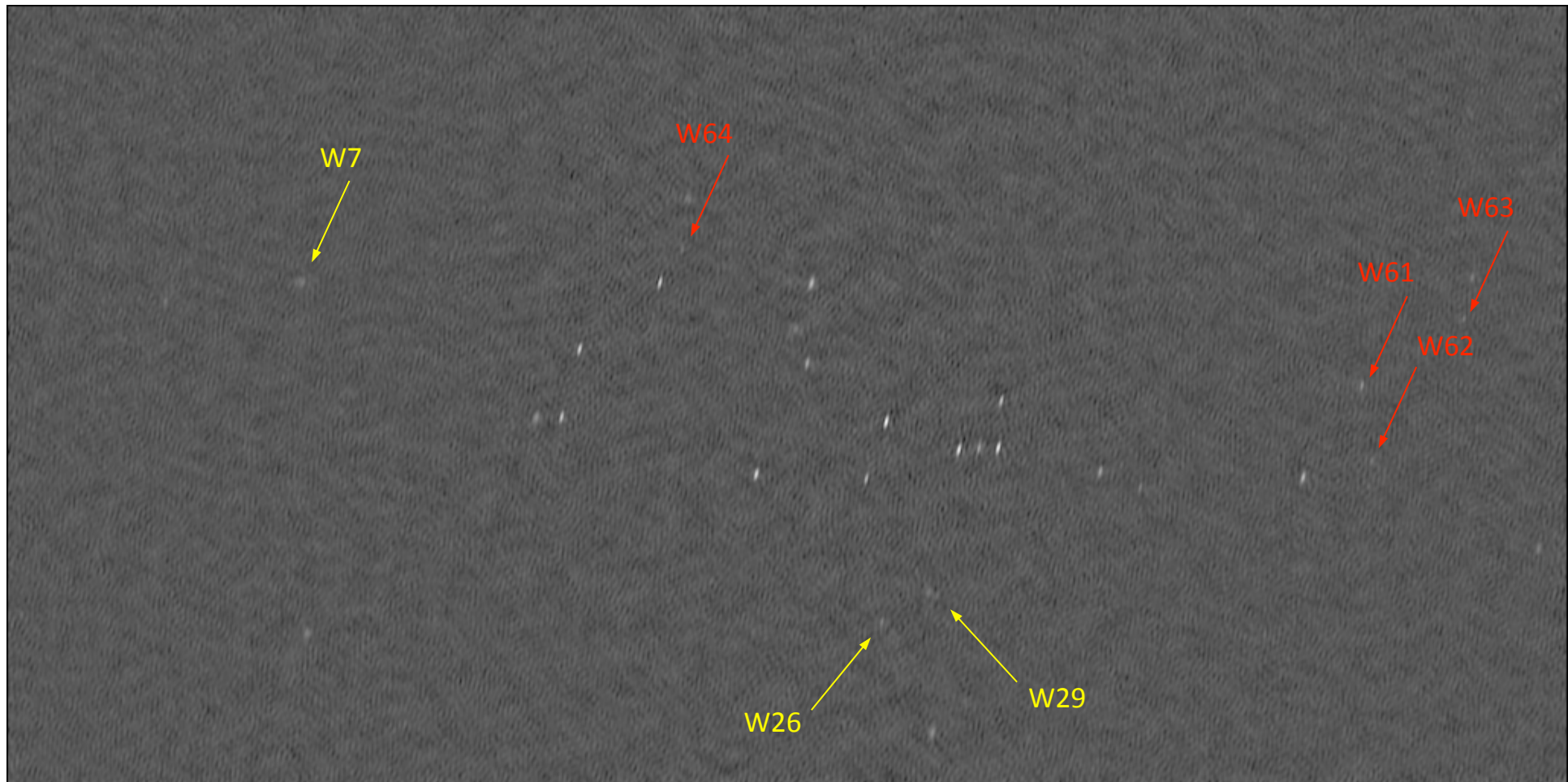
- Deep global 6cm images at three epochs on June 2008, October 2008 and February 2009.
- Look for short time variability, search for Type Ib/c supernovae, AGN, etc.
- Also combine all three epochs to make the deepest 6cm map to date .

Combined 3 epochs - East





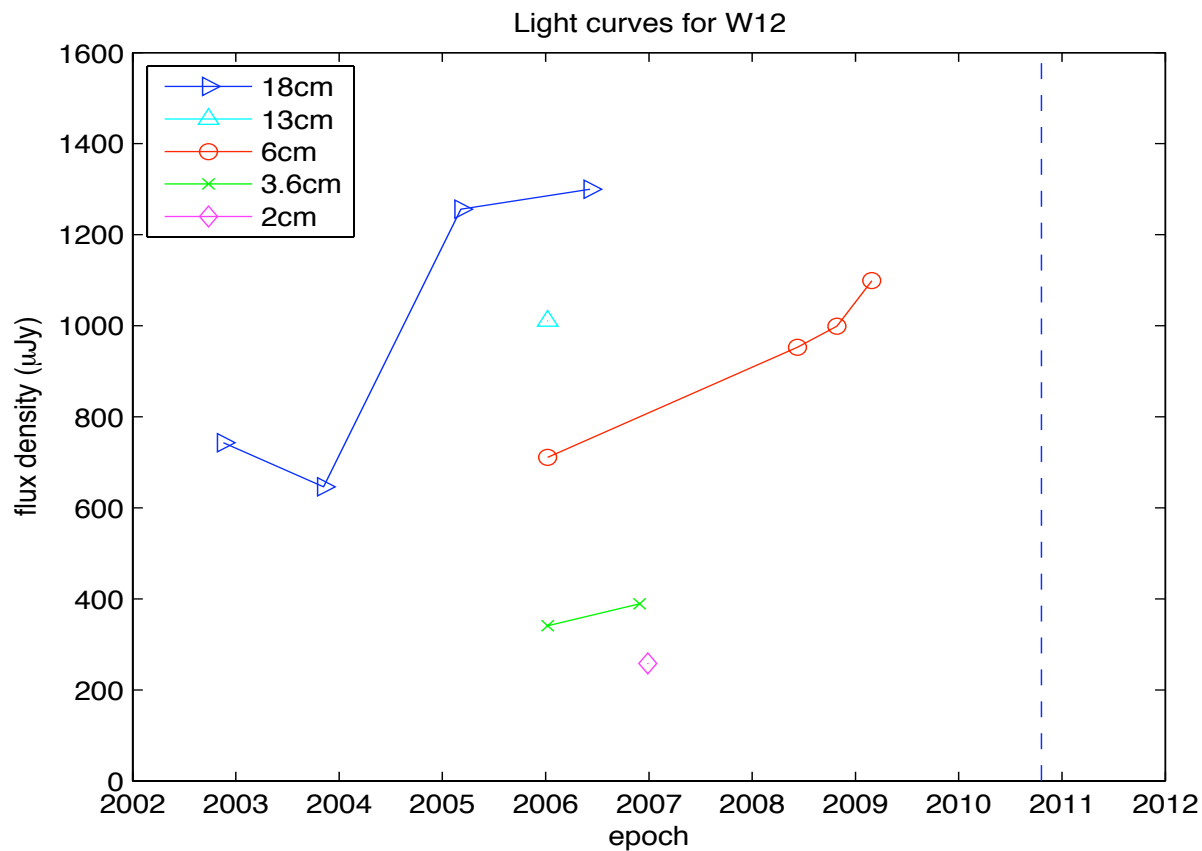
Combined 3 epochs - West



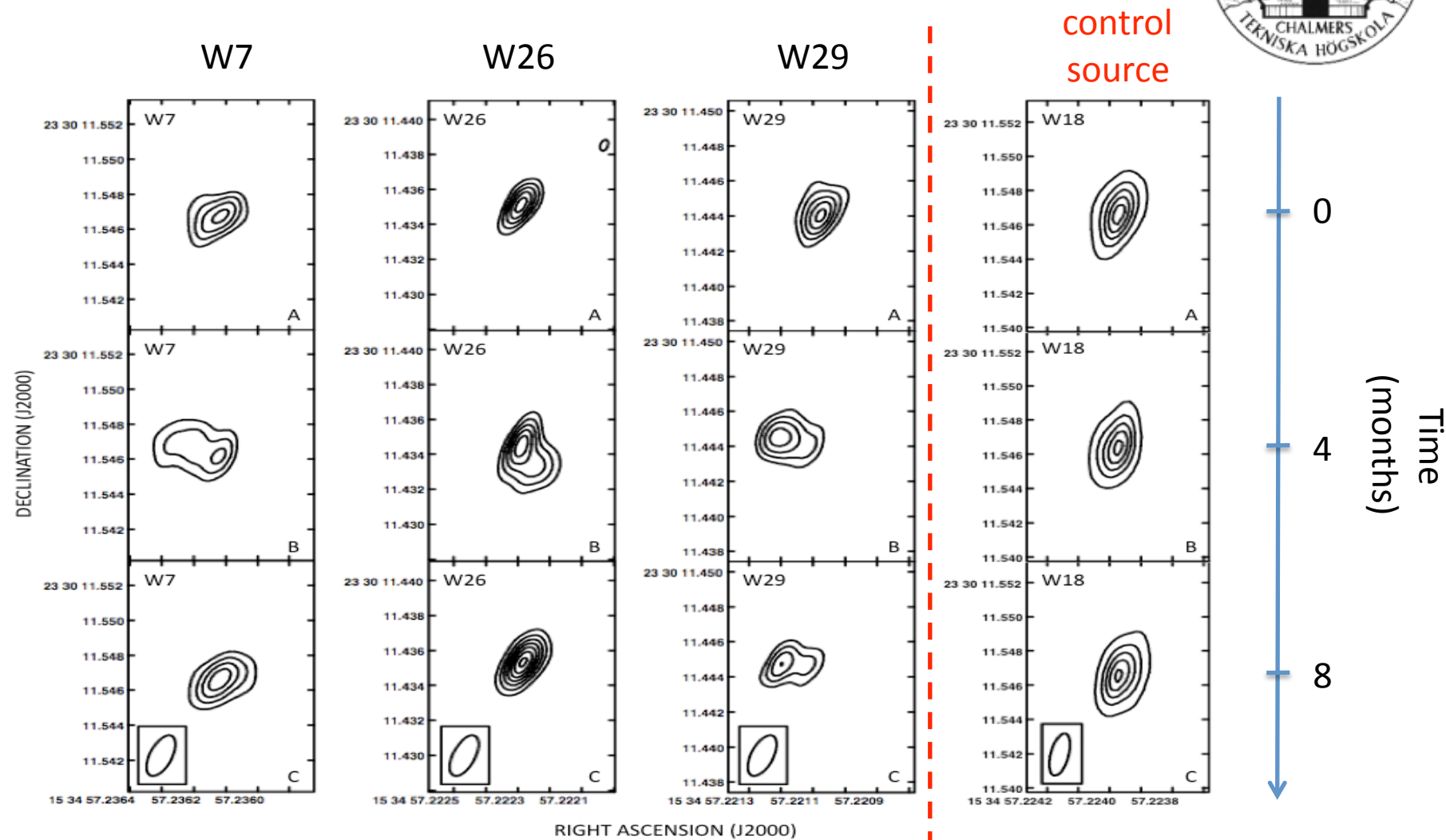
Transition object candidate W12



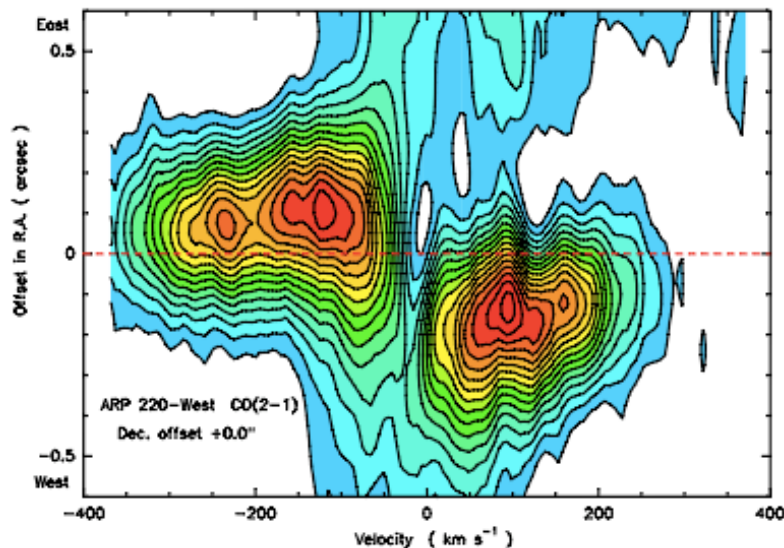
From SN to SNR?



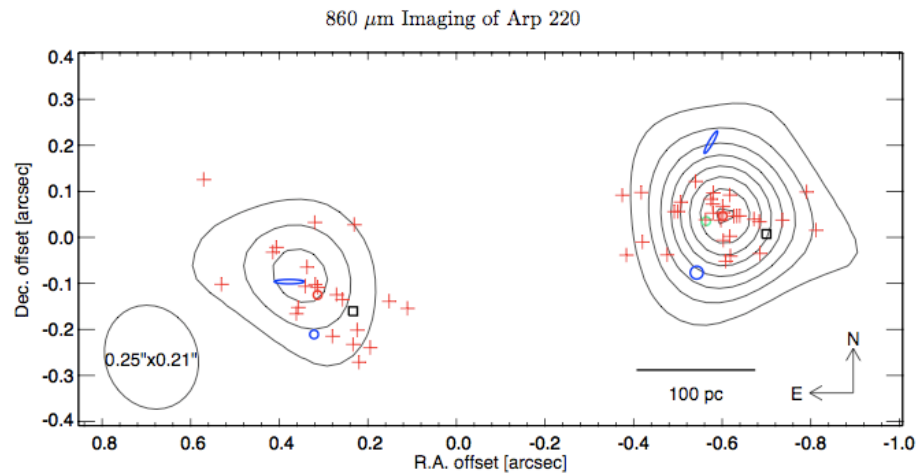
Rapidly Varying Radio Sources



Evidences for a Supermassive BH/AGN in Arp220



Downes and Ekart 2007, **dynamical evidence** for a black hole in Arp220 W. Nucleus



Sakamoto et al (2008) contours of 860 micron emission from **hot dust**. Argue too compact to be due to stars and instead black holes powered.

Rapidly Radio Variable sources in Arp220



Hot dust “AGN feature” at mm- λ

- **Green crosses:**

Downes & Eckart 2007

- **Green circle:**

Sakamoto et al 2008

- **Red diamond:**

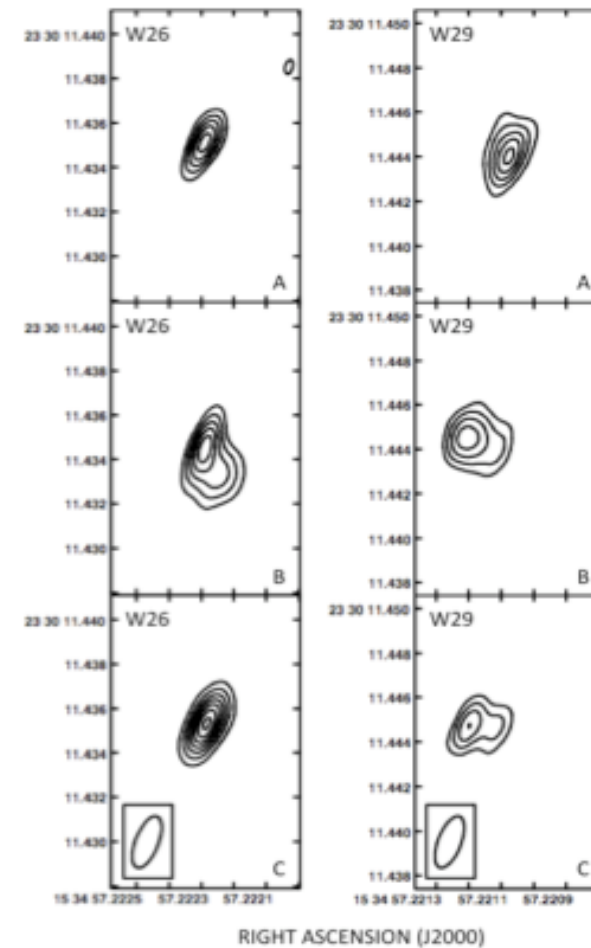
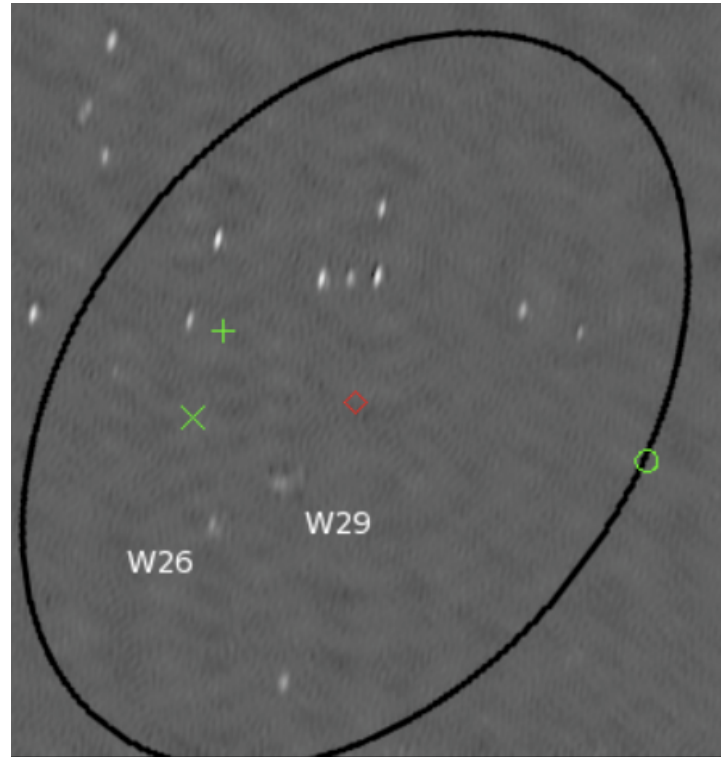
Centroid of the 3

- **Black ellipse:**

Orientation and size by D&E 07

Three global VLBI epochs combined (Batejat), one of the highest sensitivity maps ever made (5 μ Jy/beam).

Rapidly Variable Radio Sources in Arp220: potential AGN





What are they?

- Speed estimates are superluminal $4c - 12c$, similar to recent source in M82 (Muxlow et al 2010)
- Suggests a large population of objects, we are just detecting the few pointing toward us
- So what are they?
 - Supermassive black-holes / AGN?
 - Some models suggest BH in mass range 10^2 to 10^5 M_\odot form at centers of Globular / Super Star clusters, producing ‘mini-AGN’ if accreting. Arp220?
 - Micro-Quasars? (radio-jet X-ray binaries)
 - Plerions? (pulsar wind nebula)



Summary

- Compact radio sources: mixture of **SNe** and **SNR**
- **High rate** of new powerful radio SNe is hard to explain
 - very short burst viewed at right time AND a very top heavy IMF?
 - implications for theories of star formation and star-formation rate of universe?
- We **confirm Berezhko & Völk 2004 Luminosity - Diameter relation** for SNR and extend it to very young sources.
- We have possibly detected a **SN/SNR transition object**
- We have detected at least **3 highly variable sources** whose structures vary on timescales < 4 months with possible superluminal motion. No explanation yet. HSA proposal accepted.



Back-Up



Abstract

- We present multi-epoch global VLBI data at 2cm, 3.6cm and 6cm (including 3 epochs taken 4 months apart) of the compact radio sources in Arp220. We resolve many sources and estimate sizes, ages, expansion velocities and source classes. We find most source properties are consistent with them being radio supernovae or SNRs. We expand the luminosity-diameter relation for SNR to very small sources and argue this supports models where shell magnetic fields are internally amplified. We also detect one probable SN to SNR transition object candidate and three highly variable sources with possible superluminal motion (approximately $4c$) of jet-like features near rapidly varying almost stationary components. These enigmatic sources, which show similarities to the recently discovered superluminal source in M82, might be associated with an AGN or a new source class (e.g. intermediate mass black holes, microquasars or plerion powered sources).

History of ARP220 observations



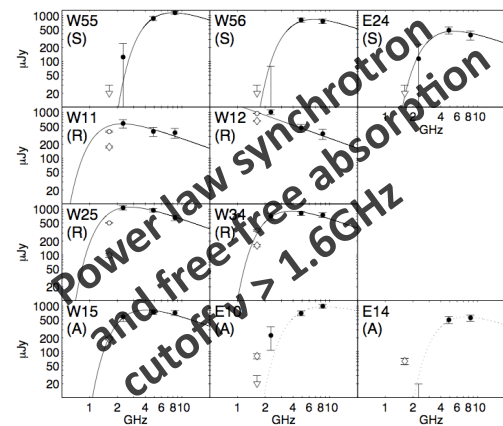
- *11.1994*: Smith et al. 1998; 18cm (global VLBI: 17 telescopes in Europe and the US, 4.2 hours integration)
- *08.1998, 04.1999, 12.1999, 06.2000*: Rovilos et al. 2003; 18cm (global VLBI)
- *11.2003*: Lonsdale et al. 2006; 18cm (global VLBI)
- *2005*: Parra et al. 2007; 6cm (Ar-Eb) (first detection <18cm)
- *01.2006*: Parra et al. 2007; 13, 6, 3.6cm (VLBA)
- *12.2006*: Conway et al. 2010 in preparation; 3.6 (VLBI), 2cm (HSA)
- *01.2006, 06.2006, 06.2008, 10.2008, 03.2009*: Batejat et al. in preparation; 6cm (global VLBI)
- *Spring 2011*: 6, 3.6, 18cm (HSA)



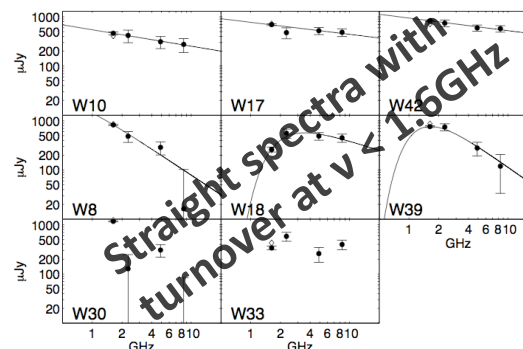
Source class

Spectra:

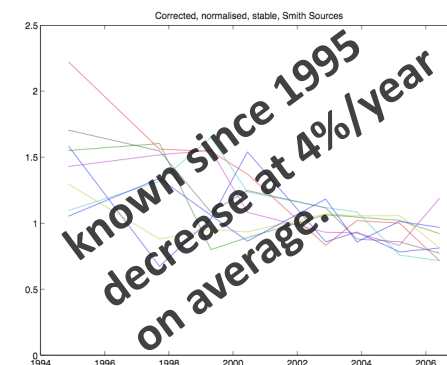
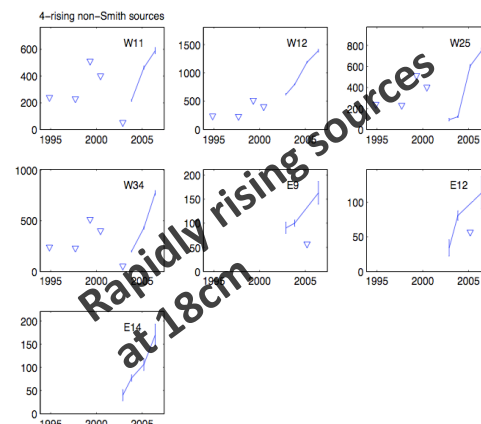
New sources



Long-lived sources



Light curves:

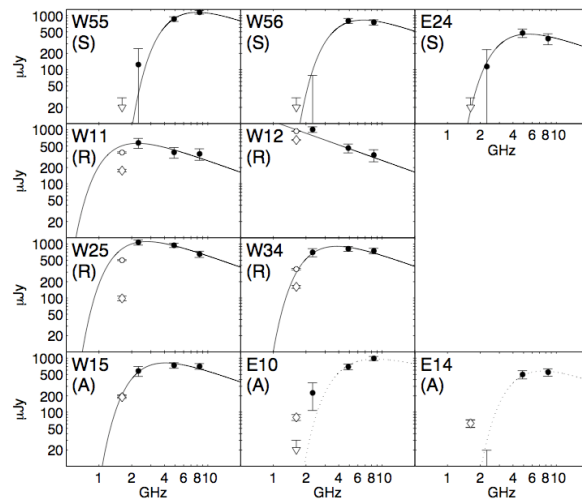




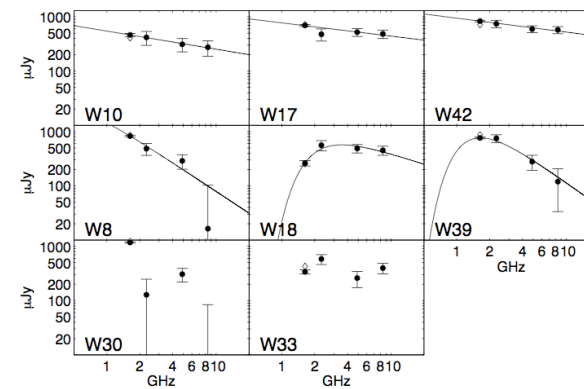
Source class

New sources

Spectra:



Long-lived sources



**Power law synchrotron
and free-free
cutoff $v > 1.6\text{GHz}$**

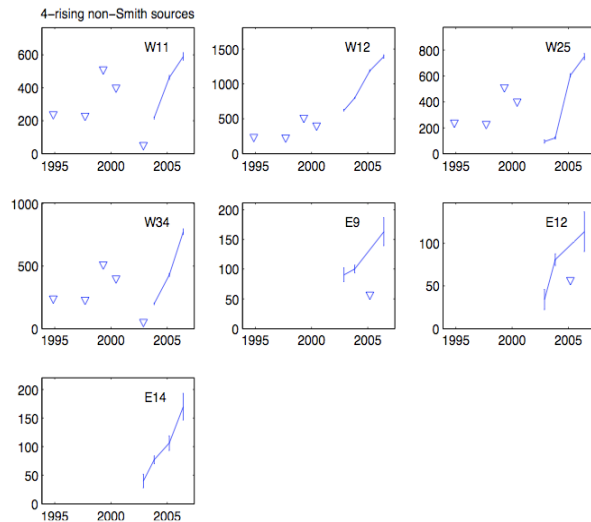
**Straight spectra with
turnover at $v < 1.6\text{GHz}$**



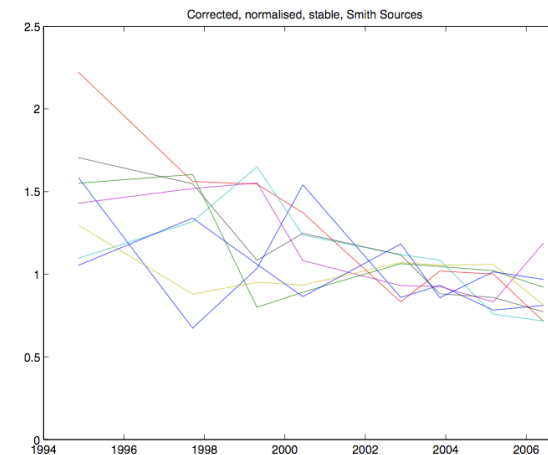
Source class

Light curves:

New sources



Long-lived sources



Rapidly rising sources
at 18cm

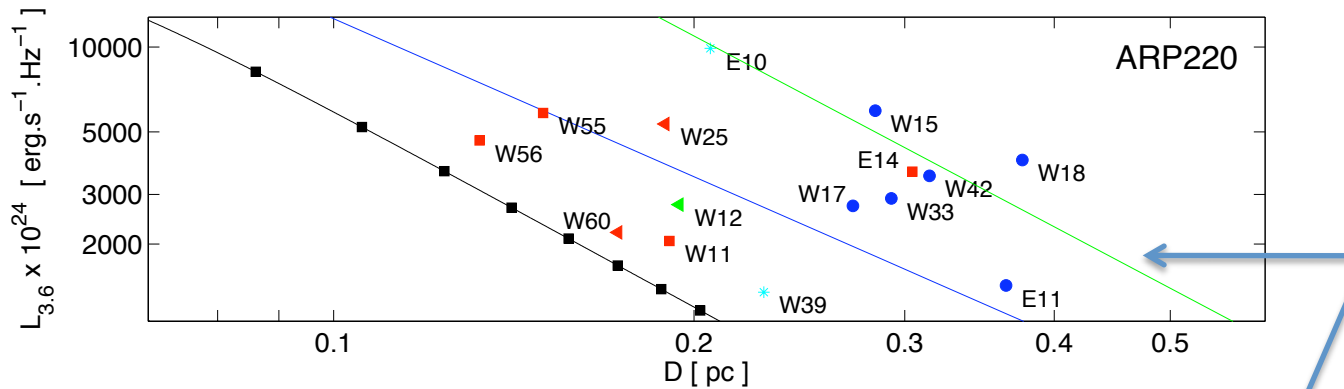
**known since 1995
decrease at 4%/year
on average**

SNR/ISM Physical Parameters

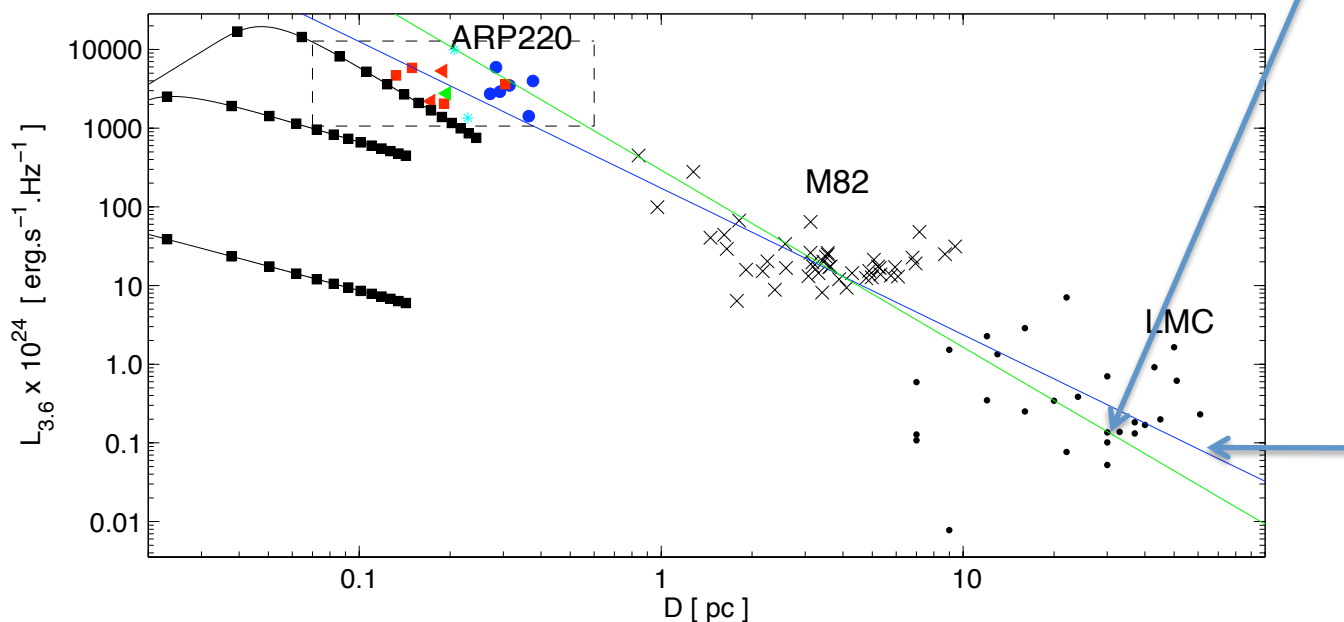


- BV04 constant (relativistic particle energy / B-field energy) - particle dominated (by factor 100). B-fields expected factor 3 lower than minimum energy estimates (gives $B=20\text{mG}$), total particle energies factor 5 larger, or 15% of kinetic energy. Total energy in electrons is 1.5% of total energy.
- Similar figures of 10% energy in protons and 1% in electrons (Laski et al 2009) needed to explain the Radio-IR correlation by calorimeter models.
- SNR luminosity decline means Internally generated B field dominates over ISM compressed one, assuming max compression ratio (of 6) ISM B-field $< 3\text{mG}$, consistent with OH Zeeman splitting observations giving $B_{ISM} = 1\text{mG}$.

Luminosity – Diameter relation

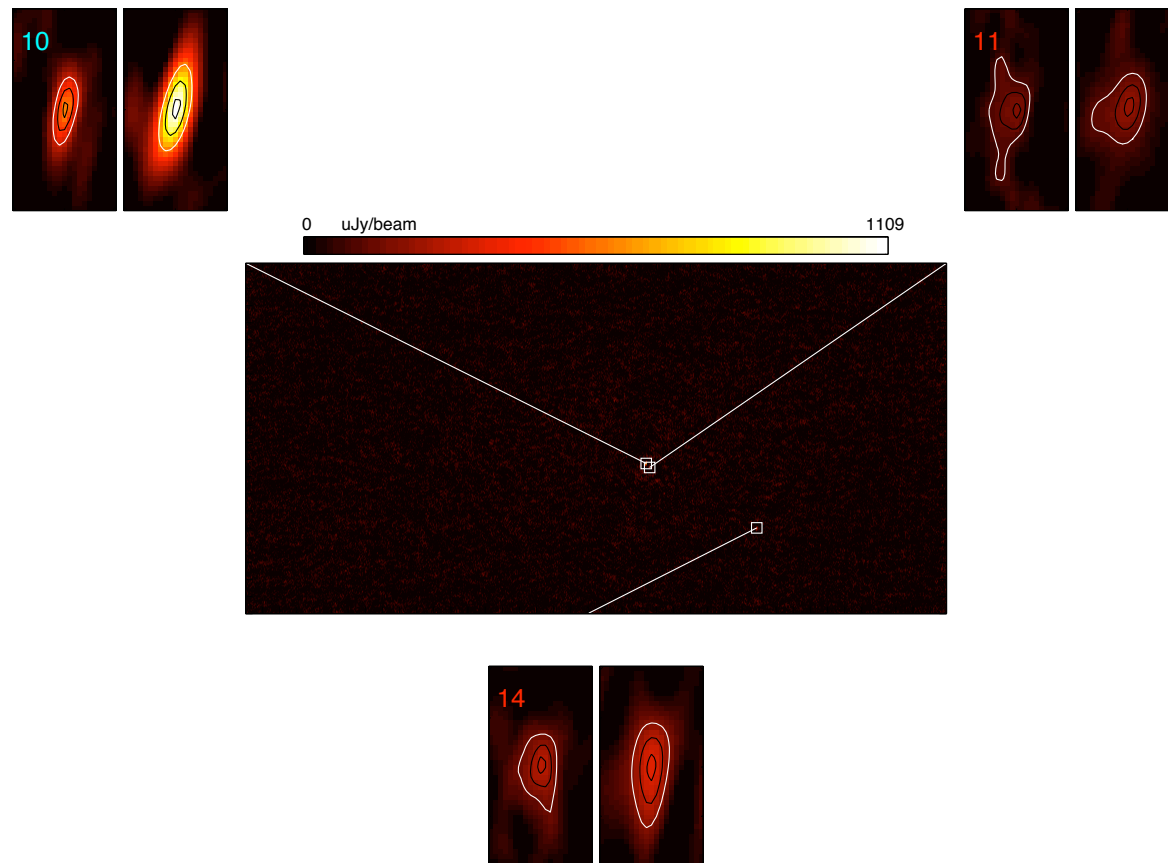


theoretical relation
of $L \propto D^{-9/4}$ for SNRs
in the Sedov phase
(Berezhko & Volk, 2004)



best fit to observations
 $L \propto D^{-1.9}$

Dec 2006, 2cm and 3.6 cm - East map (Conway et al 2010)





Berezhko and Völk (2004) model

Model of Berezhko and Völk (2004), similar to other models e.g. Huang et al (1994).
Relativistic nuclei in post shock shell in pressure balances ram pressure

$$P_c \approx \rho_{ISM} V_s^2$$

Streaming instability increases B field upstream of shock which is then compressed so that magnetic energy density in radio emitting shell

$$B^2/8\pi = 0.01 P_c$$

so $B \propto V_s$ and in Sedov phase

$$V_s \propto D^{-3/2}$$

Hence we have

$$B \propto D^{-3/2}$$



Berezhko and Völk (2004) model

Synchrotron emissivity per relativistic electron (for $\alpha = 0.5$) is

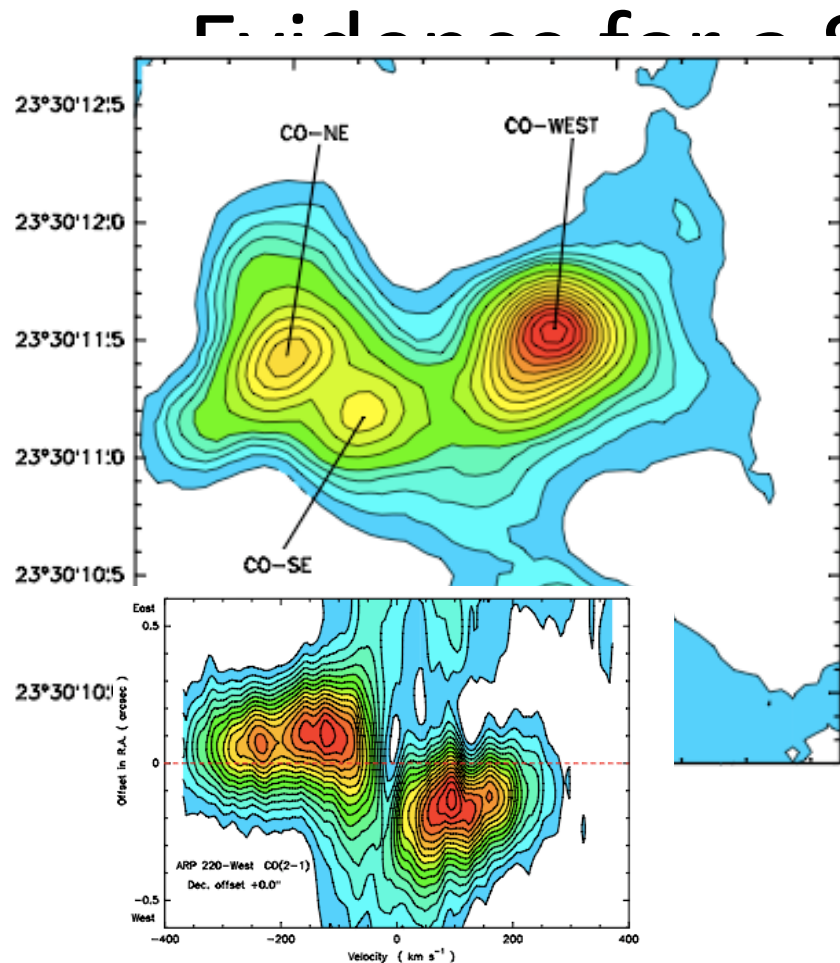
$$\epsilon \propto B^{3/2}$$

,
in Sedov phase number of relativistic electrons fixed. so radio luminosity obeys;

$$L \propto D^{-9/4}$$

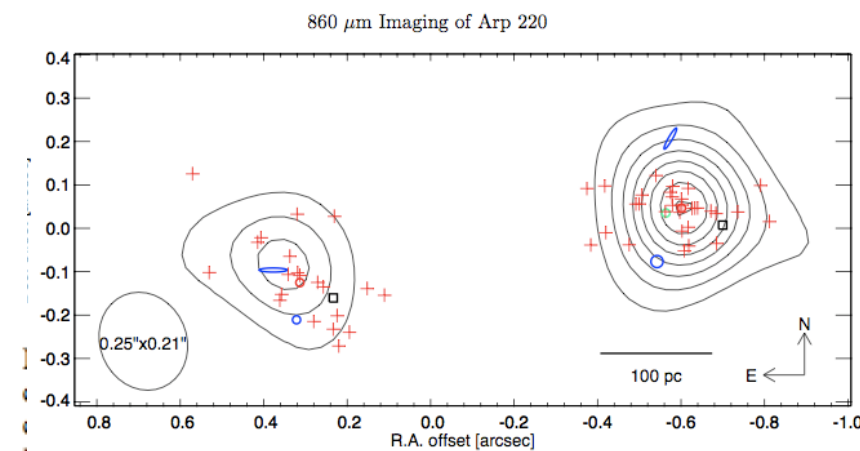
for SNR when in Sedov phase.

Alternative model presented in Thompson et al (2009), for Arp220 based on van der Laan (1963) internal B-field is just compressed B_{ISM} increased by factor 3-6- This effect dominating in Arp220 because of high ISM field.. Predicts *constant* radio luminosity versus size in Sedov phase. Can explain luminosity versus diameter between galaxies by their changing ISM density and hence ISM field - but hard to get right exponent.



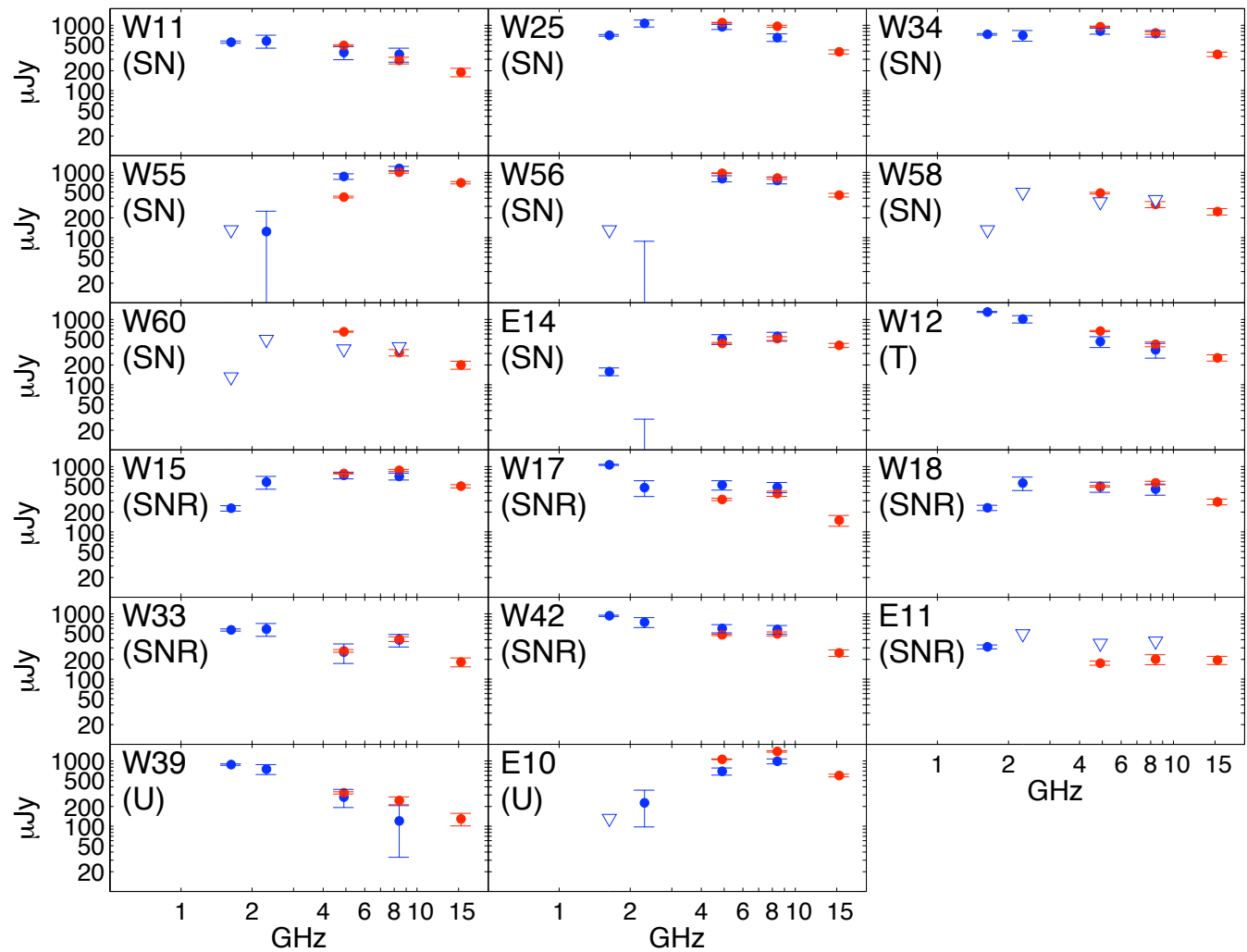
Downes and Ekart 2007,
dynamical evidence for a
black hole in Arp220 W.
Nucleus

Supermassive Arp220?



Sakamoto et al (2008) contours of 860 micron emission from hot dust, after being shifted. Argue too compact to be due to stars and instead Black holes powered.

SB in Arp220: Spectra & Class



Radiation mechanisms of SNe and SNRs

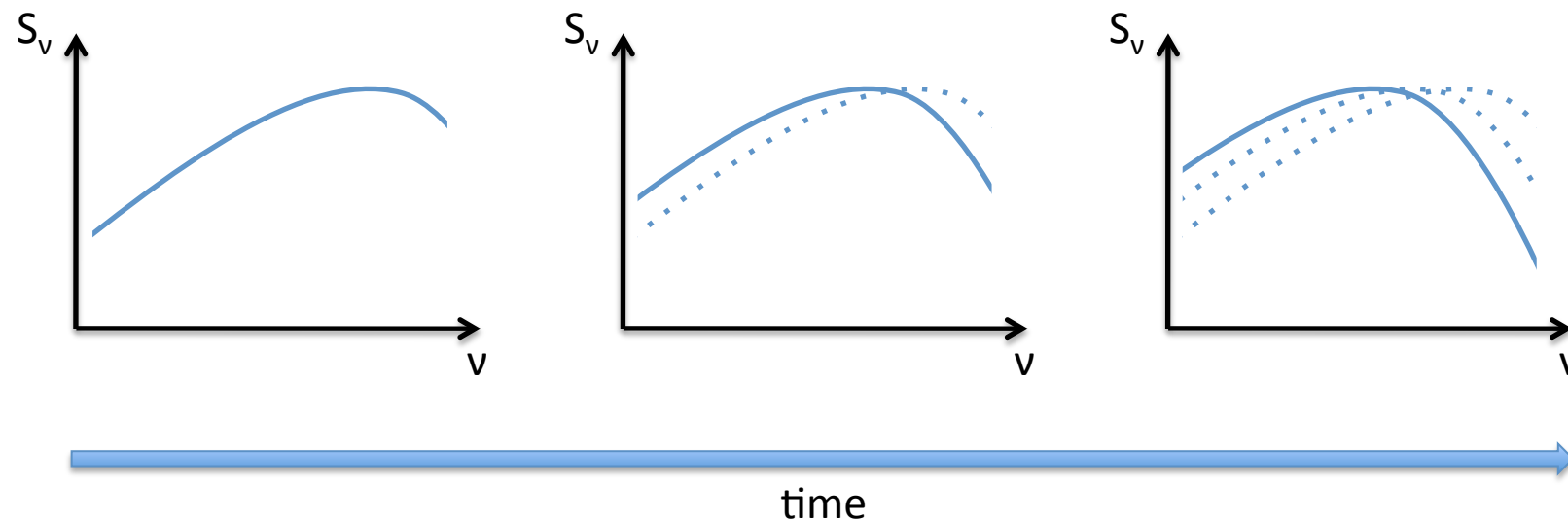


- SNe:
 - Synchrotron emission + free-free absorption
 - Absorption decreases with time
 - Radio light curves peak from higher to lower freq.
- SNRs:
 - Shockwave starts interacting with denser ISM
 - Radiates thermal X-rays and synchrotron + absorption
 - Max luminosity reached when swept-up mass = initial mass of stellar ejecta
 - then Sedov-Taylor phase

Radiation mechanisms of SNe and SNRs



- SNe and SNRs spectra:
 - well fitted by classic power law synchrotron + free-free absorption





Questions

- ARP220
 - ULIRG: closest ULIRG – IR radiations ($\sim 10^{12}$ solar luminosities) due to radiation of dust particles excited by Starburst or AGN.
 - Luminosity: $L_{\text{fir}} > 10^{12} L_{\odot}$ (fir: Far Infra-Red)
 - Distance: 77Mpc
 - 2 colliding galaxies now merging (collision started 700 M years ago)
 - Size: distance between East and West nuclei: 450pc
- The interferometer
 - Which antennas: different for each epoch
 - Longest baseline: idem
 - Beam size: (see back-up slides)
 - 2cm (U band): $1.26 \times 0.43 \text{ mas}^2$
 - 3.6cm (X band): $1.34 \times 0.56 \text{ mas}^2$
 - RMS: (see back-up slides)
 - 2cm: $\sigma_{\text{RMS}} = 28 \mu\text{Jy}/\text{beam}$
 - 3.6cm: $\sigma_{\text{RMS}} = 35 \mu\text{Jy}/\text{beam}$



Questions

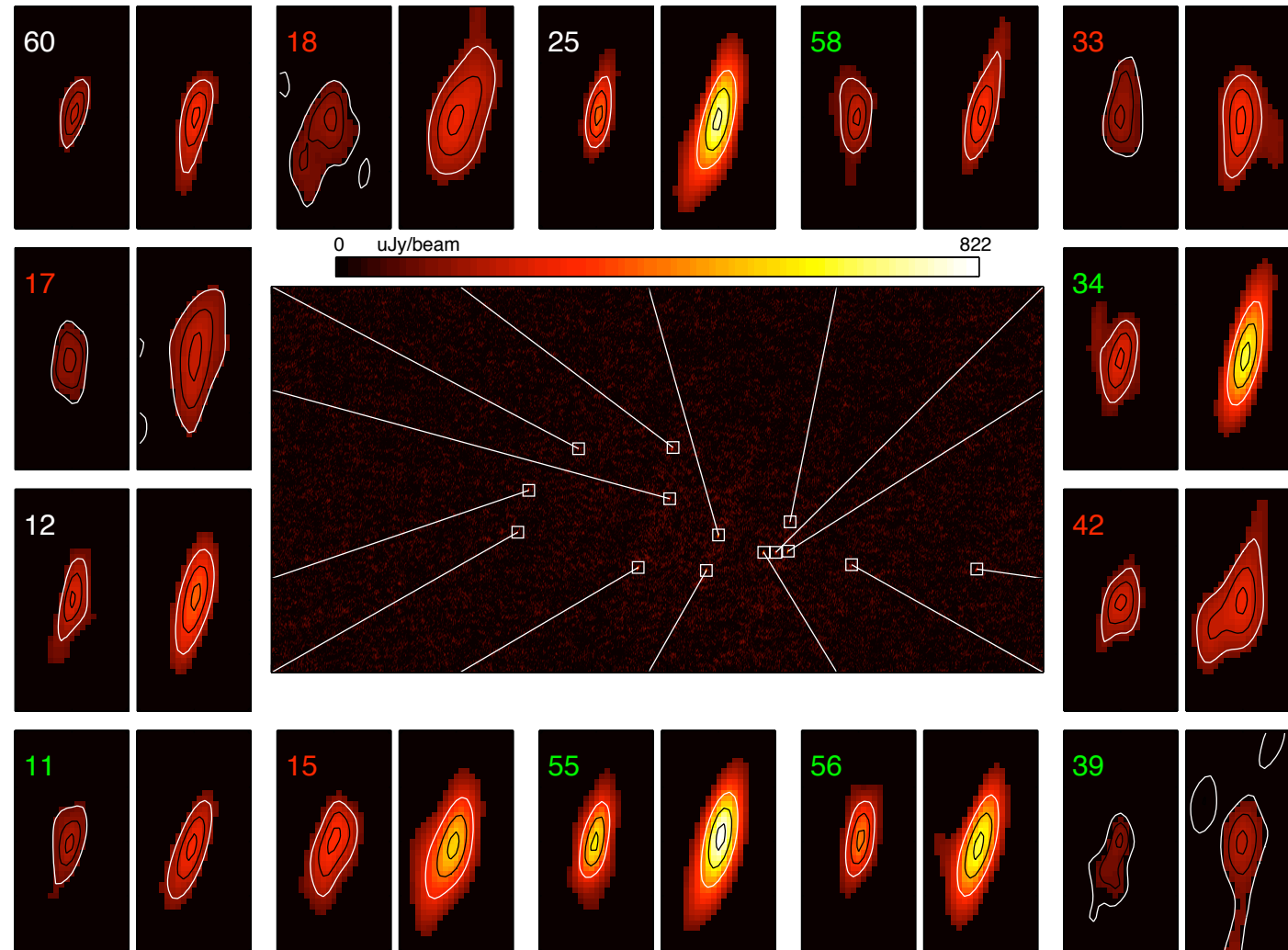
- Telescopes
 - Ef: Effelsberg (Germany)
 - Jb: Jodrel Bank (UK)
 - On: Onsala (Sweden)
 - Mc: Medicina (Italy)
 - Nt: Noto (Italy)
 - Tr: Torun (Poland)
 - Wb: Westerbork (Netherlands)
 - Sc: St. Croix (Virgin Islands)
 - Hn: Hancock (New Hampshire)
 - Ni: North Liberty (Iowa)
 - Fd: Fort Davis (Texas)
 - La: Los Alamos (New Mexico)
 - Pt: Pie Town (New Mexico)
 - Kp: Kitt Peak (Arizona)
 - Ov: Owens Valley (California)
 - Br: Brewster (Washington)
 - Ar: Arecibo (Puerto Rico)



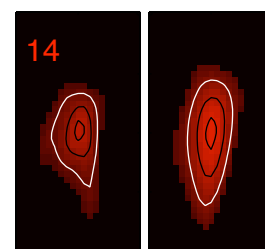
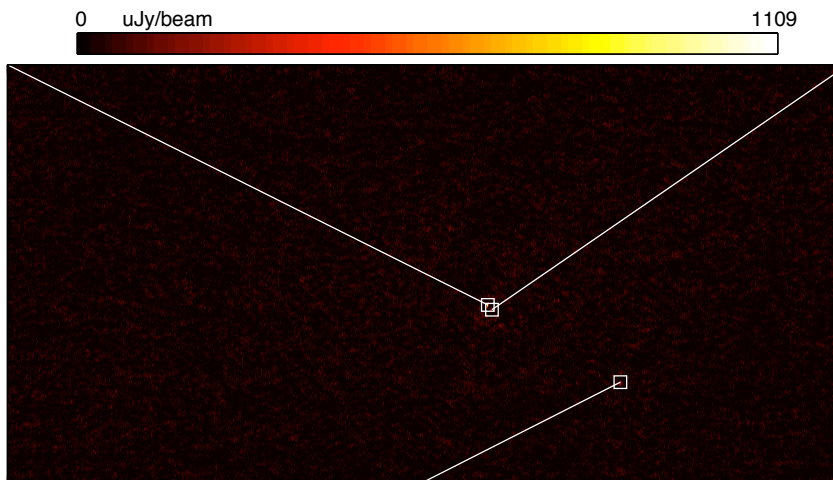
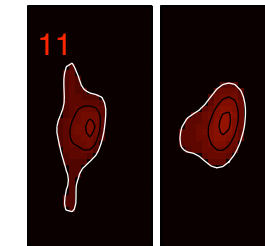
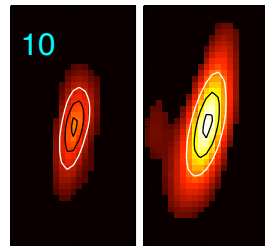
Questions

- The sources
 - Evolution at different wavelength
 - SNe:
 - Synchrotron emission produced by strong interaction between ejecta and CSM (CircumStellar Medium) and absorbed by thermal electrons. As the shock transits this ionised medium, the amount of absorption decreases (distance from shock to edge of bubble becomes shorter) → radio light curves progressively peaking from higher to lower frequencies. After peak, power law decline of flux density at each frequency.
 - SNRs:
 - When the shockwave reaches the edge of the bubble, it starts sweeping up denser ISM gas forming a shell of shocked material → SNR. When the amount of swept mass is much less than the original ejecta mass, the SNR expand at nearly constant velocity. The remnant radiates thermal X-rays and synchrotron. When the shockwave has swept the same amount of mass as the stellar ejecta, it begins to slow down and enter the Sedov-Taylor phase. At this point the remnant reaches its max luminosity and begins to cool down. The shell continues to expand and finally dilutes in the ISM.
 - Spectra:
 - in both cases well fitted by classic power law synchrotron + free-free absorption

2 and 3.6 cm, West map - blanked



2 and 3.6 cm, East map - blanked





Epoch	Code	Lamb (cm)	Array	sig_{rms} ($\mu\text{Jy.beam}^{-1}$)	Beam Size (mas 2)	Beam Size (pc)
1994.87		18	global VLBI	30	3.1 x 8.0	1.1 x 2.9

TABLE 1
HIGH FREQUENCY VLBI OBSERVATIONS OF ARP220

Epoch	Code	λ (cm)	Array	σ_{rms} ($\mu\text{Jy beam}^{-1}$)	Beam Size (mas 2)	Beam Size (pc)
2006.02	BP129	13.26	VLBA	129.54	6.6 x 3.6	2.47 x 1.35
		6.02		86.02	3.3 x 1.8	1.23 x 0.67
		3.56		86.73	3.1 x 1.7	1.16 x 0.64
2006.91	GC028	3.56	EVN	34.7	1.34 x 0.56	0.50 x 0.21
2006.99	GC028	2	VLBA	28.12	1.26 x 0.43	0.47 x 0.16



TABLE 2
PROPERTIES OF DETECTED RADIO SOURCES AND MEASURED FLUXES IN μJY

Name	SN	α_{2000} $15^{\text{h}}34^{\text{m}}...$	δ_{2000} $23^{\circ}30'$...	BP129 13 cm	BP129 6 cm	GC031A 6 cm	BP129 3.6 cm	GC028 3.6 cm peak (9)	GC028 3.6 cm integrated (10)	GC028 2 cm peak (11)	GC028 2 cm integrated (12)
(1)	(2)	(3)	(4)	(5)	(6)	(7)	(8)				
W11	...	57°2299	11''5020	572.6	382.4	491	357.5	289	279	190	163
W12	...	57°2295	11''5242	1011.4	458.1	664	341	389	416	258	253
W15	...	57°2253	11''4833	579	733.9	784	706.6	546	837	314	500
W17	6	57°2241	11''5198	477.2	520.8	314	483.9	218	385	150	134
W18	7	57°2240	11''5469	558.8	489.5	498	450.6	272	560	156	288
W25	...	57°2222	11''5005	1069.1	944	1093	648.4	752	965	390	324
W33	11	57°2200	11''4913	582.2	259.3	270	396.9	310	409	162	182
W34	...	57°2195	11''4920	698.8	813.2	953	742.8	650	758	263	358
W39	12	57°2171	11''4848	748.9	279.3	324	119.5	190	247	129	91
W42	13	57°2122	11''4824	743.1	596	476	573.7	273	492	240	251
W55	...	57°2227	11''4817	124	863.9	418	1147.3	822	1001	595	693
W56	...	57°2205	11''4913	-42.3	799	970	749.6	657	815	426	446
W58	...	57°2194	11''5075	479	...	322	296	226	250
W60	...	57°2276	11''5463	649	...	310	268	200	128
E10	...	57°2915	11''3353	227.4	692.4	1058	988.3	1109	1394	577	596
E11	...	57°2913	11''3330	175	...	201	171	165	195
E14	...	57°2868	11''2977	-100.4	498.1	430	549.2	343	509	264	400

NOTE. — COLUMNS — (1): Source names from Lonsdale et al. (2006) for all sources except W55, W56 which are from P07. Sources W58 and W60 are newly detected sources W implies source is located in the Western nucleus while E stands for East.. (2): Names used in Smith et al. (1998) and Rovilos et al. (2005). (3) and (4): J2000 Right Ascencion and Declination obtained by fitting a gaussian to the sources in the highest frequency map (U band map) . (5),(6) and (8) 13, 6 and 3.6 cm fluxes from the observations performed in experiment BP129 and presented in P07. (7): Newly acquired (epoch 2008.44) C band fluxes which will be presented and discussed in detail in Batejat et al., (in preparation). We list them at this point as they will be used to help identify sources in §4.2. (9) and (10): X band peak and integrated flux densities discussed in this paper. (11) and (12): U band peak and integrated flux densities discussed in this paper.



TABLE 3
RESULTS OF SIMULATION TO CALCULATE SOURCE DIAMETER

Source (1)	U (mas)			X (mas)			U (8)	X (9)	resolved (10)	U/X mas (11)	U/X avg pc (12)	U/X avg pc (13)
	mean (2)	min (3)	max (4)	mean (5)	min (6)	max (7)						
W11	0.255	0.143	0.361	0.197	0.100	0.327	95.2	68.8	n	0.226	0.0845	0.169
W12	0.184	0.100	0.260	0.122	0.100	0.172	88.4	24.8	n	0.153	0.0572	0.1144
W15	0.354	0.305	0.415	0.404	0.303	0.501	99.8	98.5	y	0.379	0.1417	0.2834
W17	0.320	0.201	0.440	0.406	0.215	0.581	96.3	90.5	y	0.363	0.1358	0.2716
W18	0.524	0.417	0.619	0.482	0.322	0.611	99.9	98.1	y	0.503	0.1881	0.3762
W25	0.107	0.099	0.138	0.188	0.100	0.253	33.0	72.4	n	0.1475	0.0552	0.1104
W33	0.314	0.203	0.427	0.468	0.319	0.591	96.6	97.9	y	0.391	0.1462	0.2924
W34	0.440	0.369	0.504	0.105	0.100	0.100	99.9	4.8	n	0.2725	0.1019	0.2038
W39	0.306	0.137	0.469	0.291	0.100	0.489	92.7	69.3	n	0.2985	0.1116	0.2232
W42	0.301	0.225	0.369	0.540	0.413	0.669	98.2	99.1	y	0.4205	0.1573	0.3146
W55	0.200	0.150	0.227	0.142	0.100	0.209	97.7	43.4	n	0.171	0.064	0.128
W56	0.177	0.100	0.226	0.237	0.100	0.322	92.5	87.0	n	0.207	0.0774	0.1548
W58	0.385	0.316	0.449	0.107	0.100	0.104	99.8	10.9	n	0.246	0.092	0.184
W60	0.149	0.100	0.231	0.106	0.100	0.100	64.3	9.8	n	0.1275	0.0477	0.0954
E10	0.145	0.100	0.203	0.276	0.224	0.322	83.1	97.6	n	0.2105	0.0787	0.1574
E11	0.478	0.366	0.584	0.497	0.324	0.654	99.5	97.4	y	0.4875	0.1823	0.3646
E14	0.456	0.386	0.515	0.358	0.228	0.466	99.8	95.8	y	0.407	0.1522	0.3044

NOTE. — COLUMNS — (1): Source names from Lonsdale et al. (2006) for all sources except W55, W56 which are from P07. Sources W58 and W60 are newly detected sources. (2)-(4): The mean, minimum and maximum source radius at U band as calculated by the algorithm described in §3.2.2. A * means an upper limit to the mean (see §3.2.2). (5)-(7): The mean, minimum and maximum source radius at X band as calculated by the algorithm described in §3.2.2. A * means an upper limit to the mean (see §3.2.2). (8)-(9): percentage chance of source being resolved at U band and X band respectively. We claim that a source is resolved in cases > 90%. (10) resolution at both U and X band giving a red square in 4. (11): source radius calculated by averaging value of columns 2 + 5 in mas. (12): source radius converted to parsecs where 1mas = 0.374pc at the distance of Arp220 (77Mpc). (13): source diameter in parsecs.



TABLE 4
B FIELDS AND EXPANSION VELOCITIES

Source	exp vel (Kms^{-1})	B class (mG)	B eq (mG)	B min (mG)	E mag (ergs)	E tot (ergs)
W11	26321	88.8	54	51.9	1.1E+49	1.8E+49
W12	13613	135.1	80.1	77	7.5E+48	1.3E+49
W15	33722	77.3	47.4	45.5	3.7E+49	6.5E+49
W17	42276	34.7	28.2	24.3	6.6E+48	1.2E+49
W18	15177	47.2	42.8	40.4	3.3E+49	5.7E+49
W25	13124	168.1	98.5	94.6	1E+49	1.8E+49
W33	11798	59.7	39.7	38	2.4E+49	4.3E+49
W34	31736	153.1	90.2	86.6	5.4E+49	9.5E+49
W39	9007	367.9	11.5	12.4	4.1E+50	7.2E+50
W42	12688	33.2	26.9	23.2	9.4E+48	1.6E+49
W55	64468	151.9	89.5	86	1.3E+49	2.3E+49
W56	78040	121.1	72.3	69.4	1.5E+49	2.6E+49
W58	43250	82.9	54.1	51.8	1.2E+49	2.1E+49
W60	22416	143.9	91.3	87.3	4.9E+48	8.6E+48
E10	18730	144	91.3	87.4	2.2E+49	3.9E+49
E11	43376	38.5	26.2	25.1	2E+49	3.4E+49
E14	47401	63	39.1	37.6	3.1E+49	5.4E+49



TABLE 5
SOURCE PROPERTIES THAT ARE USEFUL FOR SOURCE IDENTIFICATION

Source (1)	X change (%) (2)	C change (%) (3)	resolved at U/X (4)	spectra (5)	morphology (6)	discovered (epoch) (7)
W11	-19	28	U	plff	s	2003.85
W12	14	45	...	plff	s	2002.88
W15	18	7	U/X	plff	s	2002.88
W17	-20	-40	U/X	flat	s	1994.87
W18	24	2	U/X	plff	s	1994.87
W25	16	16	...	plff	s	2002.88
W33	3	4	U/X	flat	ix	1994.87
W34	-12	17	U	plff	iu	2003.85
W39	59	16	U	plff	iux	1994.87
W42	-14	-20	U/X	flat	iux	1994.87
W55	-28	-52	U	plff	s	2006.02
W56	-12	21	U	plff	s	2006.02
W58	U	...	p	2006.91
W60	p	2006.91
E10	41	53	X	plff	s	2002.88
E11	U/X	...	iux	2002.88
E14	-7	-14	...	plff	iu	2003.85

NOTE. — COLUMNS — (1): Source name. (2): % change in flux density at C band between epochs 2006.02 (BP129) and 2008.44 (GC031A). (3)% change in flux density at X band between epochs 2006.02 (BP129) and 2006.91 (gc028). (4): Resolved at U, X or both. (5): spectral shape; plff = power law plus free free absorption. (6): morphology; p = point like, s=shell, i=irregular. (7): epoch of discovery